220–228 Nucleic Acids Research, 2013, Vol. 41, No. 1 Published online 23 October 2012
doi:10.1093/nar/gks975

Quadruplex formation as a molecular switch to turn on intrinsically fluorescent nucleotide analogs

John Johnson[1], Robert Okyere[1], Anupama Joseph[1], Karin Musier-Forsyth[1] and Besik Kankia[1,2,*]

[1]Department of Chemistry and Biochemistry, Center for RNA Biology, the Ohio State University, Columbus, OH 43210, USA and [2]Institute of Biophysics, College of Arts and Sciences, Ilia State University, Tbilisi 0162, Republic of Georgia

Received August 16, 2012; Revised September 19, 2012; Accepted September 25, 2012

ABSTRACT

Quadruplexes are involved in the regulation of gene expression and are part of telomeres at the ends of chromosomes. In addition, they are useful in therapeutic and biotechnological applications, including nucleic acid diagnostics. In the presence of K^+ ions, two 15-mer sequences d(GGTTGGTGTGGTTGG) (thrombin binding aptamer) and d(GGGTGGGTGGG TGGG) (G3T) fold into antiparallel and parallel quadruplexes, respectively. In the present study, we measured the fluorescence intensity of one or more 2-aminopurine or 6-methylisoxanthopterin base analogs incorporated at loop-positions of quadruplex forming sequences to develop a detection method for DNA sequences in solution. Before quadruplex formation, the fluorescence is efficiently quenched in all cases. Remarkably, G3T quadruplex formation results in emission of fluorescence equal to that of a free base in all three positions. In the case of thrombin binding aptamer, the emission intensity depends on the location of the fluorescent nucleotides. Circular dichroism studies demonstrate that the modifications do not change the overall secondary structure, whereas thermal unfolding experiments revealed that fluorescent analogs significantly destabilize the quadruplexes. Overall, these studies suggest that quadruplexes containing fluorescent nucleotide analogs are useful tools in the development of novel DNA detection methodologies.

INTRODUCTION

DNA or RNA quadruplexes are involved in the regulation of gene expression (1), are present in telomeres at the ends of chromosomes (2–5) and are commonly found in DNA aptamers (6–9). Monomolecular quadruplexes are formed by stacks of G-quartets connected to each other by single-stranded loops. G-quartets are formed by four guanine residues associated in a square planar configuration, in which each guanine interacts with its two neighbors through Hoogsteen hydrogen bonds (eight per quartet). The formation of G-quartets requires the presence of cations, which bind specifically to guanine O6 carbonyl groups between the planes of the G-quartets. Because of the cation coordination and stacking interactions, monomolecular quadruplexes are remarkably stable and fold readily.

Quadruplexes possess unique optical properties in the long-wavelength range of the ultraviolet (UV) region that distinguish them from other secondary structures (10–12). Quadruplex-formation assays, which exploit this quadruplex signature to study enzymes that cleave DNA (13) or facilitate strand-exchange reactions (10), have been developed earlier. Specifically, when d(GGTTGGTGTGG TTGG), the thrombin binding aptamer (TBA) (6), is incorporated into DNA substrates, it absorbs significantly less at 300 nm than when cleaved and allowed to form a quadruplex. On enzymatic activity (i.e. strand cleavage or strand-exchange), the released sequence folds into a quadruplex and becomes visible through a spectrophotometer monitoring at 300 nm. Recently, we reported that the free energy of quadruplex formation can be used to drive isothermal amplification of DNA or quadruplex priming amplification (QPA) (14). This work used the d(GGGTG GGTGGGTGGG) (G3T) sequence, which is based on a DNA aptamer selected for binding to HIV-1 integrase (15). A key feature of QPA is that the G3T sequence is capable of forming a quadruplex with significantly more favorable thermodynamics than the corresponding DNA duplex. The primer, which is a truncated version of G3T, is designed to spontaneously fold into a monomolecular quadruplex on elongation (14). In addition, we also reported that G3T with 2-aminopurine (2AP) (Figure 1) incorporated at the fourth position demonstrated a remarkable 100-fold increase in fluorescence on quadruplex formation, which allows simple and effective quantification without extra probe molecules (14). With excitation

*To whom correspondence should be addressed. Tel: +1 614 688 8799; Fax: +1 614 688 5402; Email: kankia.1@osu.edu

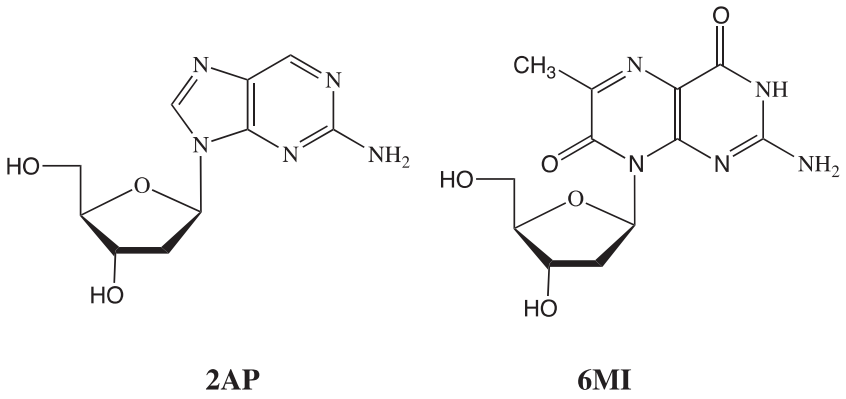

Figure 1. Structures of 2AP and 6MI.

and emission wavelengths of 310 nm and 370 nm, respectively, 2AP is a fluorescent analog of adenine, forms Watson–Crick base pairs with thymidine (16,17) and has a high quantum yield (0.68) as a free base in aqueous solutions at physiological pH (18). On incorporation into duplex structures, its fluorescence is significantly quenched, whereas partial quenching is observed even in unpaired single-stranded regions. Thus, 2AP has been widely used to study nucleic acid structures (19,20), including quadruplex loops (21–24), and to probe enzyme-induced effects on nucleic acid structure (25–27).

Another class of highly fluorescent nucleotides that are structurally similar to purines and significantly quenched by adjacent nucleotides are pteridines. There are three highly fluorescent pteridine analogs: 3-methyl isoxanthopterin (3MI) (Ex348, Em431), 6-methylisoxanthopterin (6MI) (Ex340, Em430) and 4-amino-6-methyl-8-(2-deoxy-D-ribofuranosyl)-7(8*H*)-pteridone (6AMP) (Ex330, Em435) with quantum yields of 0.88, 0.70 and 0.39 as monomers, respectively (28). 6MI is a guanine analog that perfectly base pairs with cytosine (Figure 1) (29).

In the present work, we investigated the fluorescence properties of 2AP and 6MI in loop positions of TBA and G3T. These sequences were selected because of the fact that in the presence of K^+ ions, they form monomolecular quadruplexes with different topologies. TBA folds into an antiparallel quadruplex with lateral loops (two TT and one TGT) (30–32), whereas G3T folds into a parallel quadruplex with three chain-reversal T loops (33,34) (Figure 2). The present study shows that quadruplexes are efficient scaffolds to unleash emission of fluorescent nucleotides; on quadruplex formation, the fluorescence emission of 2AP and 6MI approaches the level observed for the free nucleotides. In addition, both quadruplexes are good scaffolds for QPA primers. These studies reveal new strategies for the design of highly sensitive probes for QPA and other DNA-based diagnostics.

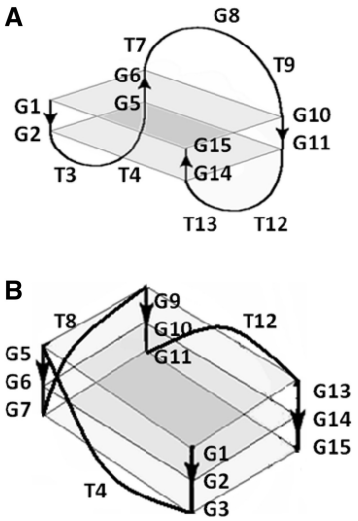

Figure 2. Schematic diagrams showing TBA (**A**) and G3T (**B**) quadruplexes. TBA folds into an antiparallel quadruplex with three lateral loops: two TT and one central TGT (A), whereas G3T demonstrates parallel topology with three chain-reversal T loops (B).

MATERIALS AND METHODS

DNA oligonucleotides (see Table 1) were obtained from Integrated DNA Technologies and Fidelity Systems. The concentration of the DNA oligonucleotides was determined by measuring UV absorption at 260 nm as described earlier (35). Unless otherwise noted, all measurements were performed in 10 mM of Tris–HCl pH 8.7, with the ionic strength adjusted by addition of appropriate salts as indicated in the figure and table legends.

To determine melting temperatures, UV absorption was recorded at either 240 nm, 260 nm or 295 nm as a function of temperature using a Varian UV–visible spectrophotometer (Cary 100 Bio). Fluorescence measurements of 2AP (Ex 310 nm, Em 370 nm) and 6MI (Ex 340 nm, Em 430 nm) were performed using a Varian spectrophotometer (Cary Eclipse). Circular dichroism (CD) spectra were obtained with a Jasco-815 spectropolarimeter. All optical devices were equipped with thermoelectrically controlled cell holders. Fluorescence quenching experiments were performed by adding aliquots of 4 M acrylamide directly into quartz cells containing oligonucleotide solutions. In a typical experiment, oligonucleotide samples were mixed and diluted into the desired buffers in optical cuvettes. The solutions were incubated at 95°C for a few minutes

Table 1. Relative fluorescence intensities (F) of 2AP and 6MI within DNA quadruplexes, and melting temperatures (T_m) and van't Hoff enthalpies (ΔH_{vH}) derived from UV unfolding profiles[a]

Oligonucleotide		F (a.u.)	T_m (°C)	ΔH_{vH} (kcal/mol)
GGTTGGTGTGGTTGG	TBA		48.0	36
GG*A*TGGTGTGGTTGG	TBA-3	28	40.5	30
GGT*A*GGTGTGGTTGG	TBA-4	1	50.0	38
GGTTGG*A*GTGGTTGG	TBA-7	70	40.0	33
GGTTGGTG*A*GGTTGG	TBA-9	1	40.5	32
GGTTGGTGTGG*A*TGG	TBA-12	32	40.0	30
GGTTGGTGTGGT*A*GG	TBA-13	1	50.0	38
GGGTGGGTGGGTGGG	G3T		90.0	64
GGG*A*GGGTGGGTGGG	G3T-*A*TT	80	85.5	54
GGGTGGG*A*GGGTGGG	G3T-T*A*T	85	85.3	55
GGGTGGGTGGG*A*GGG	G3T-TT*A*	85	84.8	55
GGG*A*GGGTGGG*A*GGG	G3T-*ATA*	174	78.5	50
GGG*A*GGG*A*GGG*A*GGG	G3T-*AAA*	240	73.5	46
GGG***G***GGGCGGGCGGG	G3T-***G***CC	67	78.0	55

[a]F values were normalized by fluorescence intensity of the G3T-*A*TT duplex; T_m values (within ±0.5°C) and ΔH_{vH} values (within ±10%) were derived from the UV melting curves at a concentration of ~4 μM per strand; TBA and variants are measured in 50 mM of KCl, 10 mM of Tris–HCl pH 8.7; G3T and variants are measured in 10 mM of KCl, 10 mM of Tris–HCl pH 8.7; italicized letters indicate the position of fluorescent nucleotides: ***A*** corresponds to 2AP and ***G*** corresponds to 6MI; in the case of TBA sequences, the number corresponds to the position of 2AP (i.e. TBA-3 has 2AP in the third position).

in the cell holder before ramping to the desired starting temperature. In the case of DNA duplexes, to ensure that the quadruplex-forming sequence formed a double helix with its complementary strand, the sequences were first annealed in CsCl- and $MgCl_2$-containing buffers. After annealing by heating at 95°C, the temperature was ramped to the desired starting temperature, KCl was added and the melting experiments were performed at a heating rate of 0.5 or 1°C/min. The melting curves allowed an estimate of melting temperature, T_m, the midpoint temperature of the unfolding process. Van't Hoff enthalpies, ΔH_{vH}, were also calculated using the following equations: $\Delta H_{vH} = 4\ R\ T_m^2\ \delta\alpha/\delta T$ in the case of monomolecular quadruplexes and $\Delta H_{vH} = 6\,R\ T_m^2\ \delta\alpha/\delta T$ in the case of bimolecular DNA duplexes, where R is the gas constant and $\delta\alpha/\delta T$ is the slope of the normalized optical absorbance or fluorescence versus temperature curve at the T_m (36).

RESULTS

CD measurements

CD spectroscopy is a sensitive technique for estimating secondary structure and folding topology of DNA quadruplexes. By comparative analysis of CD spectra and structural data of quadruplexes with T-loops, the following spectral characteristics have been observed: antiparallel quadruplexes demonstrate positive CD peaks at ~245 nm and ~295 nm and a negative peak at ~265 nm, whereas parallel quadruplexes show a strong positive band at ~265 nm and a negative peak of lesser intensity at ~240 nm (37–39). In addition, characteristics of parallel quadruplexes also include a minor positive peak at ~305 nm (37,40–42).

Figure 3A shows CD spectra of wild-type (WT) and 2AP-containing TBA quadruplexes in 50 mM of KCl, 10 mM of Tris, pH 8.7 at 20°C. Spectra are consistent with an antiparallel fold (Figure 2A), and 2AP incorporation at different positions insignificantly changes the CD profile. The spectra of WT, 2AP- and 6MI-containing G3T quadruplexes (Figure 3B) correspond to parallel folding (Figure 2B) with a negative peak at 242 nm and two positive peaks at 262 nm and 305 nm. Thus, T → 2AP or T → 6MI substitutions did not have a measurable effect on the secondary structure of either of the quadruplexes examined in this work.

Fluorescence spectroscopy

Figure 4 demonstrates fluorescence spectra of TBA (A) and G3T (B and C) quadruplexes with incorporated fluorescent nucleotides (2AP and 6MI). In the case of TBA, 2AP was incorporated into all loop positions with the exception of the central guanine in the TGT loop. This position was not altered, as (i) the central guanine is important for TBA stability (43) and (ii) we did not expect to observe significant fluorescence intensity at this position because of guanine stacking interactions with the upper G-quartet of the quadruplex (30–32). T → 2AP substitutions at positions 4, 9 and 13 resulted in efficient quenching of 2AP fluorescence to the same level as that of 2AP incorporated into the duplex DNA. In contrast, T → 2AP substitution at position 7 revealed a 70-fold increase in the fluorescence signal, whereas 2AP at positions 3 and 12 demonstrated similar ~30-fold increases (Figure 4A and Table 1). Thus, the observed fluorescence emission intensities follow the order: TBA-7 > TBA-3 ≈ TBA-12 > TBA-4 ≈ TBA-9 ≈ TBA-13. It is interesting that a similar order was observed in fluorescence quenching experiments (Supplementary Material). This latter study, which uses acrylamide as a collisional quencher, suggests that accessibility of 2AP is proportional to its fluorescence intensity.

Singe T → 2AP substitutions at all loop positions of G3T demonstrate similar (~85-fold) increases in fluorescence relative to the DNA duplex level (Figure 4B and Table 1). Thus, all loop positions in G3T reveal equal

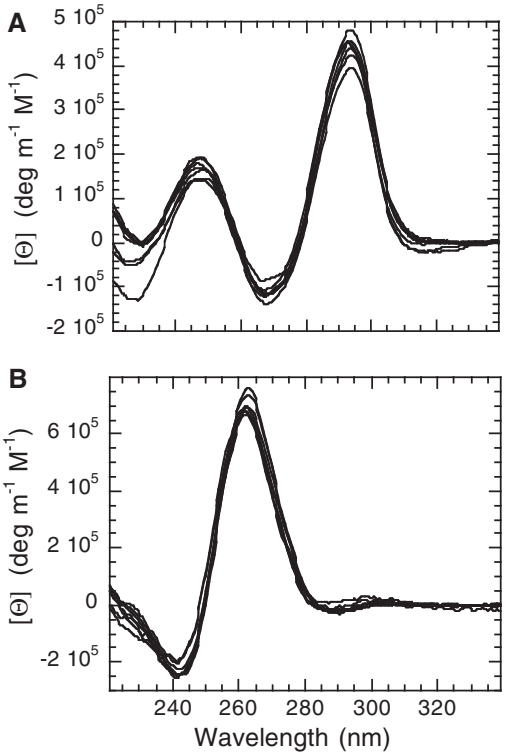

Figure 3. CD spectra of oligonucleotides with incorporated fluorescence nucleotides. (**A**) WT TBA and six variants with T → 2AP substitutions at different positions (see Table 1); (**B**) WT G3T and five variants with T → 2AP substitutions (see Table 1) and one with a 6MI nucleotide in the fourth position. All samples were in 50 mM of KCl, 10 mM of Tris–HCl pH 8.7 at 20°C.

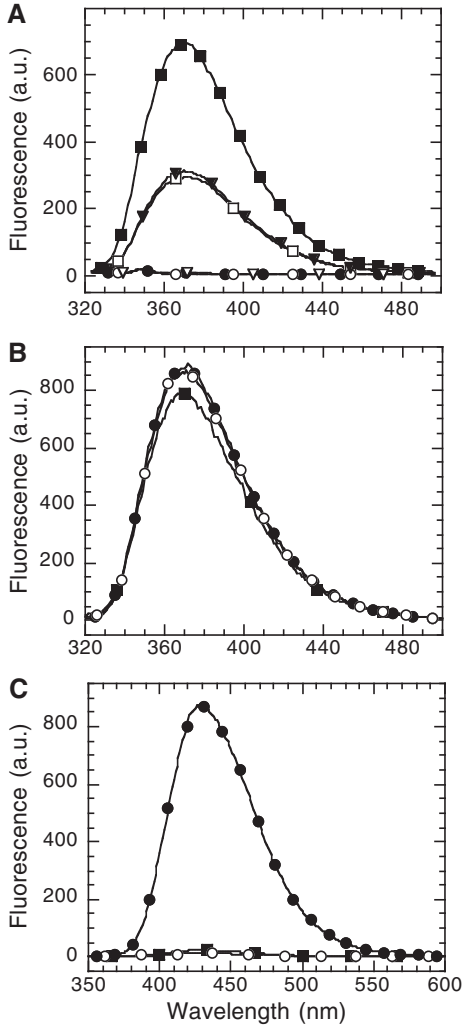

Figure 4. Fluorescence spectra of the quadruplexes with 2AP and 6MI nucleotides at different positions. (**A**) Effect of 2AP incorporation on TBA fluorescence: TBA-3 (open square), TBA-4 (filled circle), TBA-7 (filled square), TBA-9 (open circle), TBA-12 (open triangle) and TBA-13 (filled triangle). (**B**) Effect of 2AP incorporation on G3T fluorescence: G3T-***A***TT (filled square), G3T-T***A***T (filled circle) and G3T-TT***A*** (open circle). (**C**) Effects of 6MI incorporation on G3T fluorescence: G3T-***G***CC in 50 mM of KCl (filled circle), in 50 mM of CsCl (filled square) and G3T-***G***CC duplex in 50 mM of CsCl (open circle).

fluorescence effects, whereas in the case of TBA, three different fluorescence levels were observed. We also incorporated two or three 2AP nucleotides into the G3T sequence. As expected, the fluorescence intensity increased two- and three-fold, respectively, relative to the single-substituted variants (see Table 1).

To demonstrate that G3T is a suitable scaffold for other fluorescent nucleotides, we tested the highly fluorescent pteridine analog 6MI. The results of 6MI incorporation at position 4 of G3T are shown in Figure 4C, and they reveal a 67-fold increase in fluorescence on quadruplex formation.

UV unfolding experiments

Temperature-dependent unfolding of DNA duplexes is accompanied by an increase in absorbance at 260 nm, whereas quadruplexes can be monitored at several different wavelengths (10,11,44). To determine a suitable optical window for monitoring quadruplex unfolding, we recorded UV spectra of all G3T variants in the presence and absence of 15 mM K^+ ions, which revealed three main peaks around 240 nm, 260 nm and 295 nm for all oligonucleotides (data not shown). The melting profiles at these wavelengths reveal common transitions corresponding to quadruplex unfolding. As UV measurements at 295 nm are sensitive only to quadruplex unfolding (34), further UV melting experiments were performed at 295 nm. The melting profiles reveal monophasic transitions, which are characteristic of a two-state process. To confirm that the transition is monophasic, an additional dual wavelength test was performed (45). In particular, plots of the absorbance at a particular wavelength (i.e. 260 nm) versus the absorbance measured at a second wavelength (i.e. 295 nm) were linear (data not shown). This linear dependence supports the two-state nature of the transition (45).

UV unfolding experiments of TBA sequences demonstrate destabilization and stabilization effects of T → 2AP substitutions (Table 1). Substitution of 2AP at positions 3, 7, 9 and 12 is accompanied by decrease in T_m relative to WT TBA, whereas 2AP at positions 4 and 13 results in a 2°C increase in T_m. T → 2AP (Table 1) and T → 6MI (see later in the text) substitutions in G3T demonstrate destabilization effects relative to WT G3T. The van't Hoff

enthalpy, ΔH_{vH}, estimated from shape analysis for WT and variant TBA revealed values between −30 and −38 kcal/mol, which are in reasonable agreement with previously published data (43,44). The same parameter for WT and variant G3T is between −46 and −64 kcal/mol, which is also in reasonable agreement with previous measurements (34).

Fluorescence unfolding experiments

Figure 5 demonstrates fluorescence unfolding experiments of G3T sequence with 6MI in position 4 (G3T-***G***CC) and truncated variants in 15 mM of KCl, 35 mM of CsCl and 2 mM of $MgCl_2$. WT G3T-***G***CC unfolds with a T_M of ~87°C. Deletion of a single guanine at the 3′-end significantly destabilized the quadruplex (middle curve, Figure 5); however, it was still able to create some structure at lower temperatures. Deletion of two 3′-guanine nucleotides completely inhibited quadruplex formation (lower curve). The results are in good agreement with similar data obtained with G3T-***A***TT sequences (14).

The fluorescence melting of the G3T-***AAA*** and G3T-***G***CC duplexes was studied in 15 mM of KCl, 35 mM of CsCl and 2 mM of $MgCl_2$ (Figure 6). To ensure that the G3T sequences formed duplexes with their complementary strands, DNA oligonucleotides were annealed in the absence of KCl, which was added later. The heating curves (solid lines, Figure 6) reveal two separate transitions corresponding to duplex unfolding at lower temperatures and quadruplex unfolding at higher temperatures. Duplex unfolding is accompanied by an increase in fluorescence because of quadruplex formation, whereas quadruplex unfolding is accompanied by a fluorescence decrease because of 2AP and 6MI quenching by adjacent guanines in unstructured sequences. The quadruplex structure completely refolds back during the cooling process (dashed line, Figure 6). In the case of G3T-***AAA***, no duplex formation was observed (Figure 6A), whereas in the case of G3T-***G***CC (Figure 6B), ~25% of the sequences formed duplex structure on cooling.

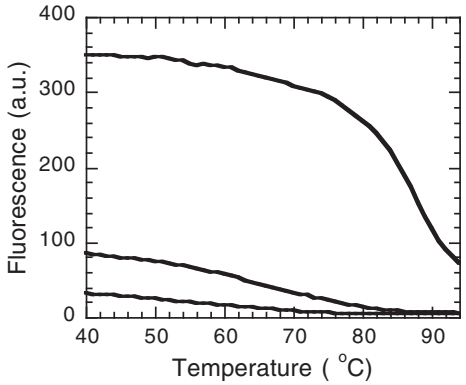

Figure 5. Fluorescence unfolding profiles of G3T-***G***CC quadruplex (upper curve) and its truncated versions missing one guanine at 3′-end (middle curve) and missing two guanines at 3′-end (lower curve) in 15 mM of KCl, 35 mM of CsCl, 2 mM of $MgCl_2$, 10 mM of Tris–HCl at pH 8.7.

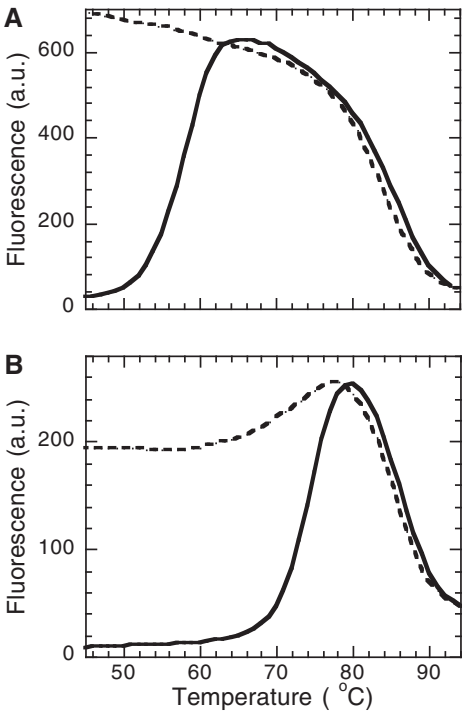

Figure 6. Fluorescence heating (solid) and cooling (dashed) curves of G3T-***AAA*** (**A**) and G3T-***G***CC (**B**) duplexes in 15 mM of KCl, 35 mM of CsCl, 2 mM of $MgCl_2$, 10 mM of Tris–HCl at pH 8.7.

DISCUSSION

Fluorescence of 2AP

The fluorescence of 2AP is sensitive to interaction with adjacent nucleotides. As a result, its high quantum yield (0.68) is reduced up to 100-fold on incorporation into a DNA duplex (18). Unfolding of the DNA double helix into unstructured single strands is typically accompanied by only a several-fold increase in fluorescence. Thus, although 2AP has the potential to be a sensitive probe, its fluorescence is significantly quenched by adjacent nucleotides even in unstructured single strands. One advantage of 2AP and other fluorescent nucleotides over externally attached tags is that they can be readily incorporated into oligonucleotides during solid-phase synthesis. Although the use of 2AP in DNA detection has been previously attempted (46,47), the sensitivity was generally believed to be insufficient for polymerase chain reaction applications. Recently, we have discovered that quadruplex formation of G3T-***A***TT is accompanied by a release of 2AP fluorescence to the same level as that of its free state, which allows accurate quantification of DNA amplicons (14). Here, we probe the effect of 2AP incorporation at different positions in the following two DNA quadruplexes: TBA, which folds into an antiparallel quadruplex (Figure 2A), and G3T, which adopts a parallel structure (Figure 2B).

2AP fluorescence in the TBA quadruplex

The emission of 2AP fluorescence tested in all T positions of TBA reveals three distinct levels (see Figure 4A and Table 1); in positions 4, 9 and 13, 2AP is efficiently

quenched to the same level as that of 2AP incorporated into DNA duplexes; in positions 3 and 12, we observe ~30-fold increase in fluorescence on quadruplex formation and the highest fluorescence signal (~70-fold increase) is observed in position 7. These results are in good correlation with structural studies (30–32). Specifically, nuclear magnetic resonance (NMR) data revealed the probable formation of a T4•T13 base pair across the G-quartet based on an observed nuclear Overhauser effect between the imino protons of these nucleotides. In addition, a nuclear Overhauser effect between the T4 and G5 and T13 and G14 imino resonances was also observed, indicating a strong stacking interaction between the T4•T13 base pair and the G-quartet (30).

X-ray crystallography also suggests formation of the T4•T13 base pair and its stacking to the G-quartet (31). Interestingly, T4 and T13 were invariant in all of the selected TBA aptamers (6), suggesting a specific role of these loop nucleotides in the quadruplex structure. The efficient quenching of 2AP nucleotides in positions 4 and 13 can be explained by formation of a 2AP•T13 base pair in TBA-4 (see Table 1) and a T4•2AP base pair in TBA-13 and their stacking to the adjacent G-quartet. The electron density of T3 and T12 was not well defined, and it was suggested that these nucleotides do not interact with the adjacent nucleotides and are accessible to the solvent (31). In agreement with these observations, our fluorescence measurements reveal significant emission of 2AP incorporated at these positions (Figure 4A and Table 1). Another interesting structural feature of TBA is that T9 interacts with the guanine of the TGT loop and the adjacent G-quartet, whereas T7 is at right angles to the G-quartet and is fully accessible to the solvent (31,32). In agreement with this structure, our measurements show the highest 2AP fluorescence signal at position 7 and complete quenching at position 9 (see Table 1).

2AP fluorescence in the G3T quadruplex

Antiparallel folding of the TBA quadruplex (Figure 2A) is a consensus of three independent structural studies (30–32), and the fluorescence data reported here are consistent with this fold. In the case of G3T, an earlier NMR study suggested that $(GGGT)_4$ possesses an antiparallel fold with two G-quartet and two T•G•T•G loops (48). However, more recent NMR (33) and thermodynamic analyses (34) are consistent with a parallel fold. In addition, incorporation of 2AP into the fourth position of G3T revealed strong fluorescence emission comparable with that of a free base (14). The latter strongly supports parallel folding of G3T with single-nucleotide chain-reversal loops, and it can be explained by completely exposing the loop nucleotide to the solvent, as both adjacent guanines of 2AP are immobilized in G-quartets without any possibility of stacking and quenching the fluorophore (Figure 2B). Note that only T → 2AP exchange in position 9 of TBA, which is completely open to the solvent (31,32), reveals comparable fluorescence effect. All other loop nucleotide exchanges in the TBA quadruplex demonstrate negligible or significantly lower fluorescence levels (see previous section).

The results reported here are also consistent with a parallel fold for G3T. As shown in Figure 4B and Table 1, T → 2AP substitutions at all loop positions of G3T demonstrate a similar ~85-fold increase in fluorescence relative to the DNA duplex level, which indicates that G3T possesses identical single nucleotide loops as shown in Figure 2B. The data are not consistent with an alternative antiparallel folding with two G-quartets with lateral GT loops based on the thermal stability of the quadruplexes. Specifically, the antiparallel quadruplex with two G-quartets revealed a T_m <50°C in the presence of 50 mM of KCl (44), whereas at the same ionic strength, G3T demonstrates unusually high stability with a T_m ≈100°C (34). Folding the antiparallel quadruplex with three G-quartets with lateral single T-loops also seems unreasonable for G3T, as (i) such loops completely inhibit quadruplex formation (43) and (ii) addition of the third G-quartet with most favorable TT and TGT loops would increase T_m only by 18°C (43). Thus, the present result, that all three T → 2AP exchanges demonstrate almost identical fluorescence effects, strongly supports parallel folding of G3T with three chain-reversal T-loops.

The fluorescence of a single 2AP can be used to monitor DNA amplification in QPA (14). The present study revealed that G3T sequences with two and three 2AP nucleotides amplify the signal further; the effect of each 2AP is additive (Table 1).

Fluorescence of 6MI in G3T

One of the most important factors limiting the yield of specific polymerase chain reaction product is the competition between primer binding and self-annealing of the product (49). An advantage of QPA primers is their self-dissociation, which allows micromolar concentrations of prode molecules to be generated (14). Thus, probe molecules in QPA have the potential to be detected by the unaided eye. However, 2AP emits at a wavelength of 370 nm, which is out of the visible range. In addition, the background fluorescence is high because of excitation in the UV range. Designing QPA probes with different emission wavelengths is also desirable for multiplex purposes. Pteridine nucleotides, such as 6MI, fluoresce in the visible range, and they are also efficiently quenched on incorporation into DNA strands (28,29). Here, we show that quadruplex formation of G3T-***G***CC is accompanied by a 68-fold increase in fluorescence (Figure 4B), which demonstrates that 6MI has the potential to be used in QPA applications.

Effect of 2AP and 6MI on stability of quadruplexes

Although thermodynamic parameters of duplexes can be estimated from nearest-neighbor analysis of equilibrium unfolding (50), effects of nucleotide exchanges in loop positions have to be experimentally determined. Thermal unfolding data for G3T sequences measured in 10 mM of KCl (Table 1) show that the single T→2AP substitution in all three positions results in similar destabilization effects, with a T_m decrease of ~5°C. The effect is proportional to the number of 2AP nucleotides incorporated (e.g. T_m of

G3T-***AAA*** is reduced to ~16°C). Single T→2AP substitutions are accompanied by an ~14% decrease in enthalpy, whereas two and three base substitutions result in a 22 and 28% decrease, respectively. Within the experimental error of ΔH_{vH} (±10%), these effects are also proportional to the number of 2AP nucleotides. This thermodynamic study is in good agreement with the fluorescence results, demonstrating the additive nature of the fluorescence of G3T with multiple 2APs. The T_m data reported here are in reasonable agreement with similar studies using $T(GGGT)_4$ sequence with loop modifications whose T → A exchanges resulted in an 8°C decrease in T_m (51).

To understand the nature of the destabilization effect of the T → 2AP substitution, initial (quadruplex) and final (unfolded single-strand) states of the unfolding process must be considered. The present fluorescence data suggest little or no interaction between the loop nucleotides and the G-quartets of folded quadruplexes. Interestingly, Rachwal *et al.* (51) found that the most stable quadruplex is formed with 1,2-dideoxyribose linkers in the loop positions, which suggested that specific interactions with the loop bases are not necessary for quadruplex formation. Thus, the T → 2AP change is not likely to affect the quadruplex structure, and the destabilization observed may be because of increased rigidity of the unfolded G3T (as purine bases are better stacking partners for guanines than pyrimidines). In other words, the destabilization effect of T → 2AP substitutions is likely to be attributed to the stronger interaction of 2AP with neighboring guanines in unstructured G3T, which has to be overcome during rearrangement of the sequence into four G-tracks to form a monomolecular quadruplex. Interestingly, A → 2AP exchanges at different loop positions in human telomere quadruplexes did not reveal any destabilization effects (24), as this substitution does not significantly alter base stacking after quadruplex formation. The latter supports our suggestion that destabilization on T → 2AP substitution is mainly because of differences in stacking interactions.

Thermal unfolding data for the G3T-***G***CC quadruplex (data not shown) measured at 10 mM of KCl revealed a 12°C and ~15% reduction in T_m and ΔH_{vH}, respectively (Table 1). The destabilization effect can be attributed entirely to T → 6MI substitution, as C nucleotides in loop positions do not have any measurable influence on the thermodynamic parameters [(51); Kankia, unpublished data]. The quadruplex destabilization effect of 6MI is significantly higher than that of 2AP or A. The stronger destabilization can be attributed to the more hydrophobic nature of 6MI, which further facilitates stacking interactions and makes quadruplex formation less favorable.

The TBA quadruplex reveals destabilization and stabilization effects on T → 2AP substitutions (Table 1). All three loop positions (3, 7 and 12) reveal an ~8°C decrease in stability relative to WT TBA (Table 1). As in the case of G3T, this can be attributed to stronger stacking interactions in the unfolded TBA sequence. The destabilization effect for TBA is stronger than the effect for G3T (8°C versus 5°C), which may be explained by significantly higher overall stability of the G3T quadruplex (T_m = 90°C) relative to TBA (T_m = 48°C) (Table 1). Interestingly, ~2°C stabilization effects were observed on substitution of positions for the positions 4 and 13 with 2AP; these nucleotides are involved in specific interactions within the quadruplex. Specifically, NMR studies reveal base pairing between T4 and T13 and strong stacking interactions between the base pair and neighboring G-quartet (30). The stabilization effect is likely because of formation of almost perfect T4•(2AP)13 or (2AP)4•T13 base pairs relative to the T4•T13 mismatch in the WT sequence. As the 2°C stabilization effect is a sum of (i) stabilization caused by T•2AP base-pairing and (ii) destabilization (~8°C) because of 2AP stacking with a neighboring guanine, we estimate 10°C as a net stabilization effect for T•2AP base-pairing.

Primer requirements of QPA

Isothermal QPA uses a primer derived from a quadruplex-forming sequence, which binds to complementary target site. Following polymerase elongation, the quadruplex forms and dissociates from the target site, which allows next round of priming without temperature cycling. In addition, the newly formed fluorescent quadruplexes should stay folded in the presence of complementary sequences. G3T-***AAA*** and G3T-***G***CC sequences, which were tested for these requirements, represent the most unstable and the most stable quadruplex structures, respectively. Fluorescence unfolding of the 15-nt G3T-***G***CC quadruplex and its truncated variants (Figure 5) demonstrates that deletion of even a single guanine inhibits quadruplex formation, as desired for QPA. However, the 14-nt primer has a higher fluorescence background (Figure 5), making the 13-nt truncated version a better primer for QPA.

The melting curve of the G3T-***AAA*** duplex reveals the following two transitions: first, duplex unfolding occurs at 57.5°C accompanied by a fluorescence increase because of quadruplex formation and then quadruplex unfolding occurs at 85.0°C (Figure 6A). The duplex unfolding temperature is significantly lower than the melting temperature of the same duplex with A•T base pairs, 69°C, estimated from nearest-neighbor analysis of equilibrium unfolding (50). The difference is likely because of (i) the destabilizing effect of 2AP•T base pairs and (ii) the presence of K^+ ions in the melting experiments (see Figure 6), which destabilize the duplex by driving quadruplex formation (14). In support of this, melting experiments of a G3T-***AAA*** duplex in the absence of quadruplex forming cation (50 mM of CsCl and 2 mM of $MgCl_2$) demonstrated a T_m of 64°C (data not shown). The cooling curve (Figure 6A, dashed line) shows that the second transition corresponding to quadruplex refolding is completely reversible; however, duplex formation is not reversible, which indicates that the complementary strand is not able to invade the already folded quadruplex even at lower temperatures. This experiment indicates that quadruplexes formed by polymerase elongation will indeed stay folded during QPA reactions, and as a result, primer binding sites will be accessible for the next primers.

The G3T-***G***CC duplex unfolds at a significantly higher temperature, 73.5°C, which is followed by immediate

quadruplex unfolding at 87.0°C (Figure 6B). The UV melting experiment of the G3T-***G***CC duplex in the absence of a quadruplex forming cation (50 mM of CsCl and 2 mM of $MgCl_2$) demonstrated a T_m of 78°C (data not shown), which reveals a 2.7°C destabilization effect of 6MI•C base pair when compared with the nearest-neighbor estimation for perfectly base paired G3T-GCC sequence under the same experimental conditions (50). The slight destabilization effect of 6MI•C base pairing agrees well with the previous reports showing that the melting temperatures of 6MI-containing duplexes are almost identical to those of control G-containing sequences (29).

The G3T-***G***CC duplex cooling curve reveals ~25% duplex refolding, which is undesired for QPA. To avoid any refolding of the G3T-***G***CC duplex, duplex and quadruplex unfolding temperatures can be separated by increasing K^+ ion concentration, which has a destabilizing effect on the G3T duplex and a stabilizing effect on the G3T quadruplexes (14). Taken together, our data suggest that both the G3T-***AAA*** sequence, containing three 2AP modifications and the G3T-***G***CC sequence having 100% GC content, can be used as primers in QPA assays.

SUPPLEMENTARY DATA

Supplementary Data are available at NAR Online: Supplementary Figure.

FUNDING

Funding for open access charge: Bill & Melinda Gates Foundation through the Grand Challenges in Global Health initiative.

Conflict of interest statement. None declared.

REFERENCES

1. Maizels,N. (2006) Dynamic roles for G4 DNA in the biology of eukaryotic cells. *Nat. Struct. Mol. Biol.*, **13**, 1055–1059.
2. De Cian,A., Cristofari,G., Reichenbach,P., De Lemos,E., Monchaud,D., Teulade-Fichou,M.P., Shin-Ya,K., Lacroix,L., Lingner,J. and Mergny,J.L. (2007) Reevaluation of telomerase inhibition by quadruplex ligands and their mechanisms of action. *Proc. Natl Acad. Sci. USA*, **104**, 17347–17352.
3. Gray,R.D., Petraccone,L., Trent,J.O. and Chaires,J.B. (2010) Characterization of a K+-induced conformational switch in a human telomeric DNA oligonucleotide using 2-aminopurine fluorescence. *Biochemistry*, **49**, 179–194.
4. McEachern,M.J., Krauskopf,A. and Blackburn,E.H. (2000) Telomeres and their control. *Annu. Rev. Genet.*, **34**, 331–358.
5. Schaffitzel,C., Berger,I., Postberg,J., Hanes,J., Lipps,H.J. and Pluckthun,A. (2001) In vitro generated antibodies specific for telomeric guanine-quadruplex DNA react with *Stylonychia lemnae* macronuclei. *Proc. Natl Acad. Sci. USA*, **98**, 8572–8577.
6. Bock,L.C., Griffin,L.C., Latham,J.A., Vermaas,E.H. and Toole,J.J. (1992) Selection of single-stranded DNA molecules that bind and inhibit human thrombin. *Nature*, **355**, 564–566.
7. Jing,N., Marchand,C., Liu,J., Mitra,R., Hogan,M.E. and Pommier,Y. (2000) Mechanism of inhibition of HIV-1 integrase by G-tetrad-forming oligonucleotides in vitro. *J. Biol. Chem.*, **275**, 21460–21467.
8. Rando,R.F., Ojwang,J., Elbaggari,A., Reyes,G.R., Tinder,R., McGrath,M.S. and Hogan,M.E. (1995) Suppression of human immunodeficiency virus type 1 activity in vitro by oligonucleotides which form intramolecular tetrads. *J. Biol. Chem.*, **270**, 1754–1760.
9. So,H.M., Won,K., Kim,Y.H., Kim,B.K., Ryu,B.H., Na,P.S., Kim,H. and Lee,J.O. (2005) Single-walled carbon nanotube biosensors using aptamers as molecular recognition elements. *J. Am. Chem. Soc.*, **127**, 11906–11907.
10. Kankia,B.I. (2004) Optical absorption assay for strand-exchange reactions in unlabeled nucleic acids. *Nucleic Acids Res.*, **32**, e154.
11. Mergny,J.L., Phan,A.T. and Lacroix,L. (1998) Following G-quartet formation by UV-spectroscopy. *FEBS Lett.*, **435**, 74–78.
12. Rachwal,P.A. and Fox,K.R. (2007) Quadruplex melting. *Methods*, **43**, 291–301.
13. Kankia,B.I. (2006) A real-time assay for monitoring nucleic acid cleavage by quadruplex formation. *Nucleic Acids Res.*, **34**, e141.
14. Kankia,B.I. (2011) Self-dissociative primers for nucleic acid amplification and detection based on DNA quadruplexes with intrinsic fluorescence. *Anal. Biochem.*, **409**, 59–65.
15. Jing,N., Rando,R.F., Pommier,Y. and Hogan,M.E. (1997) Ion selective folding of loop domains in a potent anti-HIV oligonucleotide. *Biochemistry*, **36**, 12498–12505.
16. Law,S.M., Eritja,R., Goodman,M.F. and Breslauer,K.J. (1996) Spectroscopic and calorimetric characterizations of DNA duplexes containing 2-aminopurine. *Biochemistry*, **35**, 12329–12337.
17. McLaughlin,L.W., Leong,T., Benseler,F. and Piel,N. (1988) A new approach to the synthesis of a protected 2-aminopurine derivative and its incorporation into oligodeoxynucleotides containing the Eco RI and Bam HI recognition sites. *Nucleic Acids Res.*, **16**, 5631–5644.
18. Ward,D.C., Reich,E. and Stryer,L. (1969) Fluorescence studies of nucleotides and polynucleotides. I. Formycin, 2-aminopurine riboside, 2,6-diaminopurine riboside, and their derivatives. *J. Biol. Chem.*, **244**, 1228–1237.
19. Bradrick,T.D. and Marino,J.P. (2004) Ligand-induced changes in 2-aminopurine fluorescence as a probe for small molecule binding to HIV-1 TAR RNA. *RNA*, **10**, 1459–1468.
20. Menger,M., Eckstein,F. and Porschke,D. (2000) Dynamics of the RNA hairpin GNRA tetraloop. *Biochemistry*, **39**, 4500–4507.
21. Gray,R.D., Petraccone,L., Buscaglia,R. and Chaires,J.B. (2010) 2-aminopurine as a probe for quadruplex loop structures. *Methods Mol. Biol.*, **608**, 121–136.
22. Kimura,H., Katoh,T., Kajimoto,T., Node,M., Hisaki,M., Sugimoto,Y., Majima,T., Uehara,Y. and Yamori,T. (2006) Modification of pyrimidine derivatives from antiviral agents to antitumor agents. *Anticancer Res.*, **26**, 91–97.
23. Kimura,T., Kawai,K., Fujitsuka,M. and Majima,T. (2004) Fluorescence properties of 2-aminopurine in human telomeric DNA. *Chem. Commun. (Camb.)*, 1438–1439.
24. Li,J., Correia,J.J., Wang,L., Trent,J.O. and Chaires,J.B. (2005) Not so crystal clear: the structure of the human telomere G-quadruplex in solution differs from that present in a crystal. *Nucleic Acids Res.*, **33**, 4649–4659.
25. Reha-Krantz,L.J. (2009) The use of 2-aminopurine fluorescence to study DNA polymerase function. *Methods Mol. Biol.*, **521**, 381–396.
26. Reha-Krantz,L.J., Hariharan,C., Subuddhi,U., Xia,S., Zhao,C., Beckman,J., Christian,T. and Konigsberg,W. (2011) Structure of the 2-aminopurine-cytosine base pair formed in the polymerase active site of the RB69 Y567A-DNA polymerase. *Biochemistry*, **50**, 10136–10149.
27. Tamulaitis,G., Zaremba,M., Szczepanowski,R.H., Bochtler,M. and Siksnys,V. (2007) Nucleotide flipping by restriction enzymes analyzed by 2-aminopurine steady-state fluorescence. *Nucleic Acids Res.*, **35**, 4792–4799.
28. Hawkins,M.E. (2007) Synthesis, purification and sample experiment for fluorescent pteridine-containing DNA: tools for studying DNA interactive systems. *Nat. Protoc.*, **2**, 1013–1021.
29. Hawkins,M.E. (2008) Fluorescent pteridine probes for nucleic acid analysis. *Methods Enzymol.*, **450**, 201–231.

30. Macaya,R.F., Schultze,P., Smith,F.W., Roe,J.A. and Feigon,J. (1993) Thrombin-binding DNA aptamer forms a unimolecular quadruplex structure in solution. *Proc. Natl Acad. Sci. USA*, **90**, 3745–3749.
31. Padmanabhan,K., Padmanabhan,K.P., Ferrara,J.D., Sadler,J.E. and Tulinsky,A. (1993) The structure of alpha-thrombin inhibited by a 15-mer single-stranded DNA aptamer. *J. Biol. Chem.*, **268**, 17651–17654.
32. Wang,K.Y., McCurdy,S., Shea,R.G., Swaminathan,S. and Bolton,P.H. (1993) A DNA aptamer which binds to and inhibits thrombin exhibits a new structural motif for DNA. *Biochemistry*, **32**, 1899–1904.
33. Do,N.Q., Lim,K.W., Teo,M.H., Heddi,B. and Phan,A.T. (2011) Stacking of G-quadruplexes: NMR structure of a G-rich oligonucleotide with potential anti-HIV and anticancer activity. *Nucleic Acids Res.*, **39**, 9448–9457.
34. Kelley,S., Boroda,S., Musier-Forsyth,K. and Kankia,B.I. (2011) HIV-integrase aptamer folds into a parallel quadruplex: a thermodynamic study. *Biophys. Chem.*, **155**, 82–88.
35. Kankia,B.I. and Marky,L.A. (1999) DNA, RNA, and DNA/RNA oligomer duplexes: a comparative study of their stability, heat, hydration and Mg(2+) binding properties. *J. Phys. Chem. B*, **103**, 8759–8767.
36. Marky,L.A. and Breslauer,K.J. (1987) Calculating thermodynamic data for transitions of any molecularity from equilibrium melting curves. *Biopolymers*, **26**, 1601–1620.
37. Matsugami,A., Ouhashi,K., Kanagawa,M., Liu,H., Kanagawa,S., Uesugi,S. and Katahira,M. (2001) An intramolecular quadruplex of (GGA)(4) triplet repeat DNA with a G:G:G:G tetrad and a G(:A):G(:A):G(:A):G heptad, and its dimeric interaction. *J. Mol. Biol.*, **313**, 255–269.
38. Tang,C.F. and Shafer,R.H. (2006) Engineering the quadruplex fold: nucleoside conformation determines both folding topology and molecularity in guanine quadruplexes. *J. Am. Chem. Soc.*, **128**, 5966–5973.
39. Paramasivan,S., Rujan,I. and Bolton,P.H. (2007) Circular dichroism of quadruplex DNAs: applications to structure, cation effects and ligand binding. *Methods*, **43**, 324–331.
40. Hardin,C.C., Corregan,M.J., Lieberman,D.V. and Brown,B.A. 2nd (1997) Allosteric interactions between DNA strands and monovalent cations in DNA quadruplex assembly: thermodynamic evidence for three linked association pathways. *Biochemistry*, **36**, 15428–15450.
41. Lu,M., Guo,Q. and Kallenbach,N.R. (1993) Thermodynamics of G-tetraplex formation by telomeric DNAs. *Biochemistry*, **32**, 598–601.
42. Phan,A.T., Kuryavyi,V., Ma,J.B., Faure,A., Andreola,M.L. and Patel,D.J. (2005) An interlocked dimeric parallel-stranded DNA quadruplex: a potent inhibitor of HIV-1 integrase. *Proc. Natl Acad. Sci. USA*, **102**, 634–639.
43. Smirnov,I. and Shafer,R.H. (2000) Effect of loop sequence and size on DNA aptamer stability. *Biochemistry*, **39**, 1462–1468.
44. Kankia,B.I. and Marky,L.A. (2001) Folding of the thrombin aptamer into a G-quadruplex with Sr(2+): stability, heat, and hydration. *J. Am. Chem. Soc.*, **123**, 10799–10804.
45. Wallimann,P., Kennedy,R.J., Miller,J.S., Shalongo,W. and Kemp,D.S. (2003) Dual wavelength parametric test of two-state models for circular dichroism spectra of helical polypeptides: anomalous dichroic properties of alanine-rich peptides. *J. Am. Chem. Soc.*, **125**, 1203–1220.
46. Kourentzi,K.D., Fox,G.E. and Willson,R.C. (2003) Hybridization-responsive fluorescent DNA probes containing the adenine analog 2-aminopurine. *Anal. Biochem.*, **322**, 124–126.
47. Marti,A.A., Jockusch,S., Li,Z., Ju,J. and Turro,N.J. (2006) Molecular beacons with intrinsically fluorescent nucleotides. *Nucleic Acids Res.*, **34**, e50.
48. Jing,N. and Hogan,M.E. (1998) Structure-activity of tetrad-forming oligonucleotides as a potent anti-HIV therapeutic drug. *J. Biol. Chem.*, **273**, 34992–34999.
49. Kainz,P. (2000) The PCR plateau phase—towards an understanding of its limitations. *Biochim. Biophys. Acta*, **1494**, 23–27.
50. Zuker,M. (2003) Mfold web server for nucleic acid folding and hybridization prediction. *Nucleic Acids Res.*, **31**, 3406–3415.
51. Rachwal,P.A., Brown,T. and Fox,K.R. (2007) Sequence effects of single base loops in intramolecular quadruplex DNA. *FEBS Lett.*, **581**, 1657–1660.